# A kinetic and thermodynamic understanding of $O_2$ tolerance in [NiFe]-hydrogenases

James A. Cracknell[a], Annemarie F. Wait[a], Oliver Lenz[b], Bärbel Friedrich[b], and Fraser A. Armstrong[a,1]

[a]Department of Chemistry, Inorganic Chemistry Laboratory, University of Oxford, South Parks Road, Oxford OX1 3QR, United Kingdom; and [b]Institut für Biologie/Mikrobiologie, Humboldt-Universität zu Berlin, Chausseestrasse 117, 10115 Berlin, Germany

Edited by Harry B. Gray, California Institute of Technology, Pasadena, CA, and approved September 16, 2009 (received for review May 29, 2009)

**In biology, rapid oxidation and evolution of $H_2$ is catalyzed by metalloenzymes known as hydrogenases. These enzymes have unusual active sites, consisting of iron complexed by carbonyl, cyanide, and thiolate ligands, often together with nickel, and are typically inhibited or irreversibly damaged by $O_2$. The Knallgas bacterium *Ralstonia eutropha* H16 (*Re*) uses $H_2$ as an energy source with $O_2$ as a terminal electron acceptor, and its membrane-bound uptake [NiFe]-hydrogenase (MBH) is an important example of an "$O_2$-tolerant" hydrogenase. The mechanism of $O_2$ tolerance of *Re* MBH has been probed by measuring $H_2$ oxidation activity in the presence of $O_2$ over a range of potential, pH and temperature, and comparing with the same dependencies for individual processes involved in the attack by $O_2$ and subsequent reactivation of the active site. Most significantly, $O_2$ tolerance increases with increasing temperature and decreasing potentials. These trends correlate with the trends observed for reactivation kinetics but not for $H_2$ affinity or the kinetics of $O_2$ attack. Clearly, the rate of recovery is a crucial factor. We present a kinetic and thermodynamic model to account for $O_2$ tolerance in *Re* MBH that may be more widely applied to other [NiFe]-hydrogenases.**

electrochemistry | hydrogen | hydrogenase | oxygen tolerance | *Ralstonia eutropha*

Hydrogenases play a crucial role in the metabolism of many microorganisms, where they catalyze the reversible oxidation and production of $H_2$. Hydrogenases possess active sites containing either one Ni and one Fe atom ("[NiFe]-hydrogenases"), or only Fe atoms ("[FeFe]-hydrogenases"), coordinated by cysteine thiolates and the biologically unusual ligands CO and $CN^-$. (A third class, the Hmd or [Fe]-hydrogenases (1), will not be discussed here.) Hydrogenases are highly active, with turnover frequencies for $H_2$ oxidation (believed to occur through a heterolytic cleavage mechanism) in excess of thousands of molecules of $H_2$ per second at 30° C (2). Hydrogenases are usually reported to be highly $O_2$-sensitive, being inactivated or irreversibly damaged by even trace $O_2$. It is generally considered that [FeFe]-hydrogenases react irreversibly with $O_2$, giving rise to as yet poorly characterized inactive products, whereas [NiFe]-hydrogenases react with $O_2$ to give products that can be reactivated upon reduction.

The well-characterized "standard" [NiFe]-hydrogenases from *Desulfovibrio* species, such as *Desulfovibrio fructosovorans* (*Df*), cannot oxidize $H_2$ in the presence of $O_2$. Exposure to $O_2$ under electron-rich conditions produces mainly the Ready state (also known as "Ni-B"), in which an $HO^-$ ligand is bound in a bridging position between the Ni and Fe atoms (3). This state is also produced under anaerobic oxidizing conditions, and can be rapidly recovered by applying a reducing potential under $H_2$. Exposure to $O_2$ under electron-deficient conditions produces mainly the Unready state (also known as "Ni-A"), in which a peroxo group is believed to occupy the bridging position, although other modifications may occur, such as the oxidation of sulfur ligands (3–5). Although the Unready state can be activated by applying a reducing potential under $H_2$, its recovery is many orders of magnitude slower than that of Ready. The term "$O_2$ attack" encompasses its access to the [NiFe]-active site and its subsequent reaction to form an inactive state. These reactions are summarized in Fig. 1.

In contrast with *Df* hydrogenase, the membrane-bound [NiFe]-hydrogenase (MBH) from *Ralstonia eutropha* H16 (*Re*) can oxidize $H_2$ [and, in vitro, also reduce protons to $H_2$ in the reverse reaction (6)] in the presence of air (7). As a "Knallgas" bacterium, *Re* uses $H_2$ as an alternative energy source with $O_2$ as the terminal electron acceptor. An $O_2$-tolerant hydrogenase is therefore essential for this metabolic pathway of energy conservation and, more generally, would be crucial for other microorganisms oxidizing $H_2$ in environments where $O_2$ may be found.

Protein film electrochemistry (PFE) has proved especially useful in probing the reactions of hydrogenases in air (2). In this technique, small amounts of enzyme are adsorbed onto an electrode such that they retain native catalytic activity. Catalytic activity is proportional to the electrical current, and is directly controlled through a precisely applied electrode potential. A key advantage of PFE over solution techniques, especially when measuring enzyme activity in air, is that soluble electron donors/acceptors (which invariably react with $O_2$) are not required. By using PFE, we recently showed that the $O_2$ tolerance of the MBH enzyme from *Ralstonia metallidurans* CH34 (*Rm*, closely related to *Re*) is so effective that the oxidation of even nM levels of $H_2$ in air can be detected (8), consistent with the very low threshold limits for $H_2$ uptake determined by Conrad et al. (9). A practical demonstration of $O_2$ tolerance was provided by a membraneless fuel cell producing power from 3% $H_2$ in air (10, 11).

Crystallographic and computational studies have suggested that hydrophobic "gas channels" provide a selective filter to restrict the access of small molecules such as $O_2$ and CO in hydrogenases (3). Duche et al. (12) reported how enlarging the gas channel in the regulatory hydrogenase from *Rhodobacter capsulatus* increased its $O_2$-sensitivity. We used a similar strategy with *Re* MBH, anticipating that a restricted gas channel would make the enzyme even more $O_2$ tolerant; however, no such effect was observed. Clearly, gas channels alone cannot confer $O_2$ tolerance. Most significantly, recent EPR and FTIR studies on *Re* MBH showed that reaction with $O_2$ even under electron-deficient conditions produces only the Ready state; no Ni-A (Unready) was detected (13).

In this paper, we describe PFE studies on *Re* MBH that offer valuable insight into the kinetic and thermodynamic aspects of $O_2$ tolerance and support a model that may be generally useful.

## Results

**Defining an $O_2$ Tolerance Factor.** We measured the inhibitory effect of $O_2$ on $H_2$ oxidation activity over a wide range of pH values,

Author contributions: J.A.C. designed research; J.A.C. and A.F.W. performed research; J.A.C. and A.F.W. analyzed data; and J.A.C., A.F.W., O.L., B.F., and F.A.A. wrote the paper.

The authors declare no conflict of interest.

This article is a PNAS Direct Submission.

[1]To whom correspondence should be addressed. E-mail: fraser.armstrong@chem.ox.ac.uk.

This article contains supporting information online at www.pnas.org/cgi/content/full/0905959106/DCSupplemental.

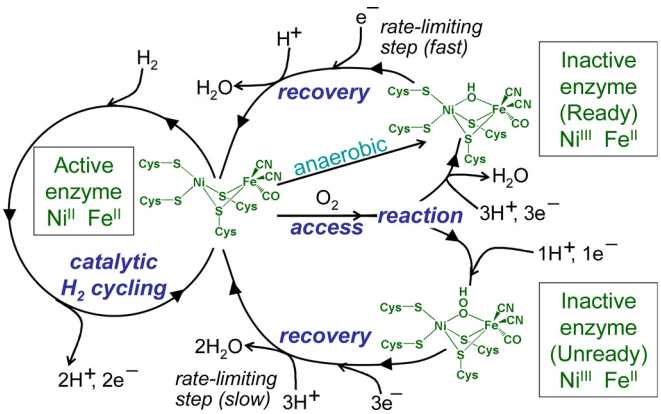


**Fig. 1.** A simplified scheme showing the reactions of standard [NiFe]-hydrogenases. Active hydrogenase molecules catalyze $H_2/H^+$cycling, and are subject to aerobic inactivation, forming either the Ready or Unready forms, depending on the availability of electrons and protons. The Ready form can also be formed anaerobically at oxidizing potentials. (Adapted from ref. 20 with permission from the Royal Society of Chemistry.)

$O_2$ concentrations, electrode potentials, and temperatures. From these measurements, we obtained values for the "$O_2$ tolerance factor," $K_I^{O_2,app}$, by using the method described previously (14, 15). The $O_2$ tolerance factor is the $O_2$ concentration required to attenuate $H_2$ oxidation activity by 50%; therefore, a high value indicates a high level of $O_2$ tolerance. The $H_2$ oxidation current at a pyrolytic graphite "edge" (PGE) electrode modified with *Re* MBH was monitored following a succession of injections of $O_2$ gas into the electrochemical cell headspace. After correcting for film loss over time, $K_I^{O_2,app}$ was obtained by analyzing the catalytic current that stabilizes at each $O_2$ concentration. Details are provided in *Methods* and values are summarized in Table 1. Significantly, $O_2$ tolerance increases with decreasing electrode potential (i.e., more reducing conditions) and with increasing temperature. It appears that $K_I^{O_2,app}$ may decrease at high pH, but we were unable to extend the pH range studied as the enzyme activity became too low. These observations suggest immediately that $O_2$ tolerance does not rely on a selective filter, such as a restrictive gas channel.

**Table 1. Values of $K_I^{O2,app}$ under a range of conditions**

| Variable | $K_I^{O2,app}$, μM |
|---|---|
| Potential, V vs. SHE* | |
| −0.018 | 1,630 |
| +0.052 | 390 |
| +0.122 | 110 |
| +0.192 | 40 |
| +0.262 | 8 |
| pH† | |
| 4.5 | 70 |
| 5.0 | 80 |
| 5.5 | 110 |
| 6.0 | 90 |
| 6.5 | 70 |
| Temperature, ° C‡ | |
| 10 | 70 |
| 20 | 70 |
| 30 | 110 |
| 40 | 140 |

*All values were recorded at pH 5.5, 30° C.
†All values were recorded at 30° C, at a constant overpotential (driving force) of +453 mV relative to the thermodynamic $H^+/H_2$ cell potential at each pH.
‡All values were recorded at pH 5.5, at a constant overpotential (driving force) of +453 mV relative to the thermodynamic $H^+/H_2$ cell potential at each temperature.

**Table 2. Values of $K_M^{H2}$ under a range of conditions**

| Variable | $K_M^{H2}$, μM |
|---|---|
| Potential, V vs. SHE* | |
| −0.158 | 8 |
| −0.058 | 6 |
| +0.042 | 14 |
| +0.142 | ≈100 |
| +0.242 | ≈130 |
| pH† | |
| 4.5 | 6 |
| 5.0 | 8 |
| 5.5 | 6 |
| 6.0 | 15 |
| 6.5 | 10 |
| Temperature, ° C‡ | |
| 10 | 0.4 |
| 20 | 1 |
| 30 | 6 |
| 40 | 24 |

*All values were recorded at pH 5.5, 30° C.
†All values were recorded at 30° C, at a constant overpotential (driving force) of +273 mV relative to the thermodynamic $H^+/H_2$ cell potential at each pH.
‡All values were recorded at pH 5.5, at a constant overpotential (driving force) of +273 mV relative to the thermodynamic $H^+/H_2$ cell potential at each temperature.

**Michaelis Constants for $H_2$.** The $O_2$ tolerance of a hydrogenase in $H_2$ oxidation is expected to depend on the enzyme's affinity for $H_2$ because of competition for binding at the active site. We define $K_M^{H2}$ as the Michaelis constant for $H_2$. We used the method described previously (14, 15) to determine $K_M^{H2}$ for *Re* MBH over a range of pH, potentials, and temperatures (Table 2). A known volume of $H_2$-saturated buffer solution was introduced into the electrochemical cell, and the $H_2$ was then removed by a constant flow of inert gas, typically $N_2$. Values of $K_M^{H2}$ were determined by analyzing the current vs. time trace as described in refs. 14 and 15.

**Rates of $O_2$ Reaction.** The rate of reaction of $O_2$ at the active site of *Re* MBH was probed by analyzing the current decay following $O_2$ introduction at a range of potentials, pH, and temperatures. A typical experiment is shown in Fig. 2*A*. An electrode modified with *Re* MBH was placed in a gas-tight electrochemical cell under an atmosphere of 50% $H_2$ and 50% $N_2$. The electrode was initially polarized at −0.508 V to ensure that all of the enzyme was active. After 120 s, the potential was stepped to the value at which the rate of $O_2$ reaction was to be determined. After allowing a background current to be determined, the atmosphere was changed to 50% $H_2$, 25% $O_2$, and 25% $N_2$; simultaneously, an aliquot of temperature-equilibrated buffer solution, saturated with 50% $H_2$ and 50% $O_2$ was injected into the cell solution. Under the experimental conditions, the mixing time is ≈0.1 s and therefore insignificant on the experimental timescale. The decrease in current that begins immediately is purely due to $O_2$ reaction at the active site; at the potentials used, direct $O_2$ reduction at the electrode surface is negligible, and, crucially, following the introduction of $O_2$, neither $H_2$ nor $O_2$ concentrations change over the course of the measurement. After correcting data for anaerobic inactivation and film loss (Fig. 2*A*), the rate of $O_2$ reaction was determined (Fig. 2*B*). Typically, the reaction was first order for more than two half-lives, and rate constants are presented in Table 3 (see also Table S1 of the *SI*

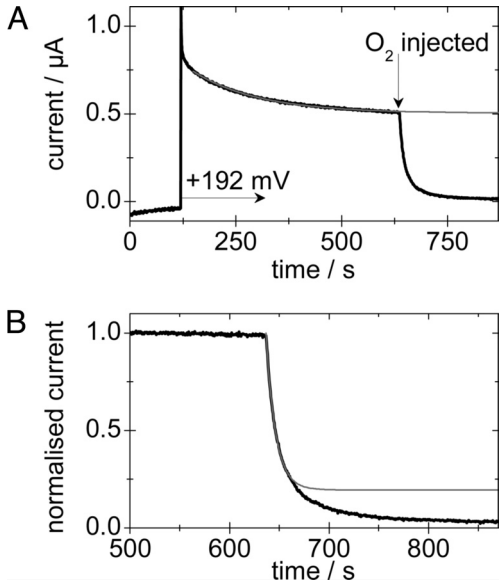


**Fig. 2.** A typical experiment to determine the rate of $O_2$ reaction with *Re* MBH. (*A*) The current vs. time trace (black) with the fit to film loss/anaerobic inactivation (gray). (*B*) The corrected data (black), with the fit to the initial attack by $O_2$ (gray). Experimental conditions were pH 5.5, 10° C, +0.192 V, electrode rotation rate = 4,500 rpm.

*Appendix*; trends within sets of experiments are independent of the method used to determine the rates).

The temperature dependence of the rate constants gave a linear fit to the Eyring equation with an activation enthalpy of ≈34 kJ mol$^{-1}$. We also measured the rate of $O_2$ reaction with the $O_2$-sensitive [NiFe]-hydrogenase from *Desulfovibrio gigas* by using the same method; a rate of 0.73 s$^{-1}$ was calculated at pH 6.5, 10° C, +0.192 V.

**Rates of Reactivation.** Rate and potential dependencies of recovery from both anaerobic and aerobic inactivation were measured at 10° C (the rate of recovery at 30° C is so rapid that *Re* MBH regains full activity within the "dead time" caused by the release

**Table 3. Calculated rates of reaction of $O_2$ (25%) with *Re* MBH under a range of conditions, electrode rotation rate = 4500 rpm**

| Variable | Rate of $O_2$ reaction, s$^{-1}$ |
|---|---|
| Potential, V vs. SHE* | |
| +0.192 | 0.11 |
| +0.262 | 0.10 |
| +0.332 | 0.10 |
| +0.402 | 0.11 |
| pH† | |
| 4.5 | 0.12 |
| 5.5 | 0.11 |
| 6.5 | 0.11 |
| Temperature, ° C‡ | |
| 0 | 0.06 |
| 10 | 0.11 |
| 20 | 0.19 |
| 30 | 0.31 |

*All values were recorded at pH 5.5, 10° C.
†All values were recorded at 10° C, at a constant overpotential (driving force) of +523 mV relative to the thermodynamic $H^+/H_2$ cell potential at each pH.
‡All values were recorded at pH 5.5, at a constant overpotential (driving force) of +523 mV relative to the thermodynamic $H^+/H_2$ cell potential at each temperature.

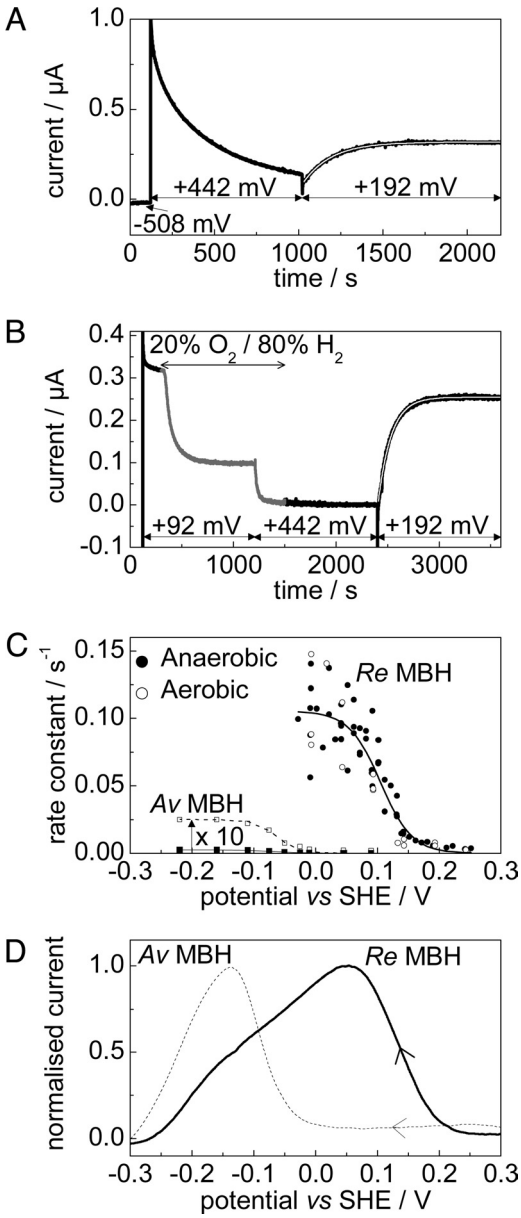


**Fig. 3.** Reactivation of aerobically and anaerobically inactivated states of *Re* MBH. (*A* and *B*) Typical experiments to measure the rate of reactivation of *Re* MBH under 100% $H_2$ following anaerobic (*A*) and aerobic (*B*) inactivation. In these examples, reactivation was measured at +0.192 V. (*C*) Rates of reactivation as a function of potential with a fit to the data overlaid. Data for the reactivation of *Av* MBH from the Unready state (filled squares, taken from reference 16, pH 6, 45° C) are also shown, and have been multiplied by 10 for clarity (unfilled squares). Sigmoidal fits are also shown. (*D*) Voltammograms (100% $H_2$, 0.1 mV s$^{-1}$) of *Re* MBH (bold) and *Av* MBH (dashed), showing recovery after aerobic inactivation at 392 mV under $N_2$. All at pH 5.5, 10° C, electrode rotation rate = 2,500 rpm.

of electrode capacitive charge). To measure the rate of recovery after anaerobic inactivation, an electrode modified with *Re* MBH was placed in a gas-tight cell under a constant flow of $H_2$. After 120 s at −0.508 V, the electrode was stepped to a high potential (+0.442 V), causing the enzyme to anaerobically inactivate. After 900 s, the electrode was stepped to the potential at which the rate of recovery was to be measured. A single exponential was fitted to the current vs. time trace (Fig. 3*A*; data from the first 10 s following the potential step were within the dead time and thus not included).

Experiments to measure the rate of reactivation following aerobic inactivation were more complex (Fig. 3*B*). Again, the electrode was held, initially, for 120 s at −0.508 V under 100% $H_2$. The potential was then stepped to +0.092 V. (At this potential, anaerobic inactivation is negligible.) The cell headgas was then changed from 100% $H_2$ to 80% $H_2$ and 20% $O_2$, causing the current to decrease as the enzyme becomes aerobically inactivated. After 900 s, the current reaches a plateau level, at which point the electrode potential was stepped to +0.442 V and the headgas changed back to 100% $H_2$. At this potential, the enzyme does not reactivate, thus allowing a clear time window for gas exchange. After 900 s (to ensure that all $O_2$ was removed from solution), the electrode was stepped to the potential at which the rate of recovery was to be measured, and the rate of reactivation was determined by fitting a single exponential as before.

Fig. 3*C* compiles the rates of reactivation following both anaerobic and aerobic inactivation, plotted as a function of potential. The rate of recovery is similar in each case, and a limiting rate of *ca.* 0.1 $s^{-1}$ is reached at potentials below 0 V. Fitting the data to a sigmoid gives the number of electrons involved in the reactivation process, $n$ (16). The best fit to the data yields $n = 0.96$ (overlaid in Fig. 3*C*), consistent with a single electron transfer. Also overlaid in Fig. 3*C* are the rates of recovery at 45° C of the Unready state of the $O_2$-sensitive MBH from *Allochromatium vinosum* (*Av*) (data from ref. 16). The Unready state is produced in large amounts under similar conditions in *Av* MBH. Reactivation of *Re* MBH following aerobic inactivation is clearly much faster than that of *Av* MBH. (Note that Ready and Unready reactivate at similar potentials in *Av* MBH.)

Potentials of reactivation are most easily compared by using voltammetry. Fig. 3*D* shows reactivation of both *Re* MBH and *Av* MBH after aerobic inactivation, recorded under the same conditions. The MBH-modified electrode was initially held at −0.558 V under 100% $N_2$. The potential was then stepped to +0.392 V and an aliquot of $O_2$-saturated buffer was simultaneously injected into the cell solution, causing the enzyme to inactivate aerobically. After 300 s, the headgas was changed to 100% $H_2$; then, after 900 s, the potential was slowly (0.1 mV $s^{-1}$) swept back to −0.558 V, allowing the recovery to be monitored. Reactivation of *Av* MBH occurs at a much lower potential, requiring ≈200 mV extra driving force compared to *Re* MBH.

## Discussion

PFE allows the detailed measurement of reactions crucial to understanding $O_2$-tolerant $H_2$ oxidation in [NiFe]-hydrogenases. The $O_2$ tolerance factor, $K_I^{O_2,app}$, depends strongly on electrode potential and temperature but is not affected by pH in the region 4.5–6.5. Greatest $O_2$ tolerance is observed at low potentials and, significantly, at high temperatures. Standard $O_2$-sensitive [NiFe]-hydrogenases typically have values of $K_I^{O_2,app}$ that are very low. For example, under one bar $H_2$, *Av* MBH is completely inhibited by just 4 μM $O_2$ (+0.142 V, pH 5.6, 30° C) (7), and the soluble hydrogenase from *Df* is completely inhibited by 5 μM $O_2$ (+0.190 V, pH 7, 40° C) (14)—thus, even micromolar $O_2$ concentrations are well in excess of $K_I^{O_2,app}$ for these enzymes. By contrast, for *Re* MBH, $K_I^{O_2,app}$ is ≈50 μM at these conditions and exceeds 1.6 mM at −0.018 V. To deconvolute the $O_2$ tolerance factor, it is necessary to probe the potential, pH, and temperature dependencies of the various contributory reactions and incorporate these within a model. Specifically, we are inspecting whether the individual reactions that must form the basis of $O_2$ tolerance either support, oppose, or are indifferent to the potential and temperature dependencies of $K_I^{O_2,app}$.

We first consider $H_2$ cycling in the absence of $O_2$, where both the affinity for $H_2$ and the catalytic turnover frequency ($k_{cat}$) are crucial. Although it has not yet proved possible to determine $k_{cat}$ for *Re* MBH electrochemically, it is likely, by analogy with other [NiFe]-hydrogenases, that *Re* MBH has a turnover frequency for $H_2$ oxidation in the order of $10^3$ $s^{-1}$ at 30° C (17).

The Michaelis constant for $H_2$, $K_M^{H_2}$, increases with increasing electrode potential and increasing temperature. The smaller is $K_M^{H_2}$, the more long-lived is the Michaelis complex ($E_{act}-H_2$, where $E_{act}$ represents Active hydrogenase), and hence the more likely the hydrogenase should be protected against $O_2$ binding at the active site. This is indeed the case for the potential dependence but not for the temperature dependence, showing that $K_M^{H_2}$ cannot be the dominating factor in determining $O_2$ tolerance. Consistent with this, $K_M^{H_2}$ values for *Re* MBH at low potentials are similar to those determined for some $O_2$-sensitive hydrogenases, such as *Av* MBH and the soluble enzyme from *Df* [which has $K_M^{H_2} \approx 5$ μM at −0.16 V (14)]. In addition, some mutants of *Re* MBH exhibit a very high $K_M^{H_2}$ but retain substantial $O_2$ tolerance (15).

There is a natural potential dependence in $K_M^{H_2}$, because the rate of catalysis ($k_{cat}$, *cf.* Eq. **2**, below) increases with increasing driving force (a consequence of the inherent high activity of the active site and the limit on how fast electrons can be supplied from the electrode). This dependence is evident in voltammograms for numerous hydrogenases catalyzing $H_2$ oxidation (2, 18). (Interestingly, low $H_2$ concentrations also increase the extent of anaerobic inactivation, potentially leading to small overestimates in $K_M^{H_2}$.) An increase in $K_M$ with increasing temperature is a typical trend and has origins in the increase in $k_{cat}$ and, in this case, the increasing rate of anaerobic inactivation with increasing temperature.

The rates of reaction of *Re* MBH with $O_2$ (Fig. 2) are unaffected by changing potential or pH but increase strongly with increasing temperature. If the rate of $O_2$ attack (which includes its transport through the protein) were a controlling factor in determining $K_I^{O_2,app}$, then at higher temperatures the hydrogenase would be less $O_2$-tolerant, which is not the case. The lack of a pH- or potential-dependence in the rate of reaction with $O_2$ is in excellent agreement with the findings of Léger et al. (14) in their studies on *Df* hydrogenase. The potential dependence of $K_I^{O_2,app}$ does not therefore arise from a dependence in the rate of $O_2$ reaction. It is worth noting, however, that the rates of $O_2$ reaction for *Re* MBH are considerably lower than for the periplasmic hydrogenase from *D. gigas*, whose catalytic subunit shares 67% sequence identity with the large subunit of *Df* hydrogenase.

We finally turn to the properties of the reactivation reaction. Our electrochemical results support the spectroscopic evidence that, in contrast with standard $O_2$-sensitive hydrogenases, *Re* MBH makes only the Ready state on reaction with $O_2$: No detectable amounts of Unready are made. All data fitted well to a single exponential, showing that only one inactive state is being recovered (recovery of *Av* MBH, which produces both Ready and Unready states, is biphasic). The rates of recovery of *Re* MBH following both anaerobic and aerobic inactivation cannot be distinguished, suggesting strongly that the same state is formed regardless of whether the active site is oxidized by $O_2$ or anaerobically at high potential. As expected, rates increase with increasing temperature (18). The value of $n$ (the number of electrons involved in the reductive reactivation of inactive $Ni^{III}$ to an active $Ni^{II}$ state) is 0.96, implying a single electron transfer consistent with reactivation of Ready (Fig. 1). The potential of reactivation of *Re* MBH is more than 200 mV more positive than for the $O_2$-sensitive [NiFe]-hydrogenases from *Av* and *D. gigas* (18), and reactivation is therefore thermodynamically more favorable. [Interestingly, in the soluble hexameric $NAD^+$-reducing [NiFe]-hydrogenase from *Re*, the inactive Ready state can be reactivated by using reducing equivalents from added NAD(P)H (19).]

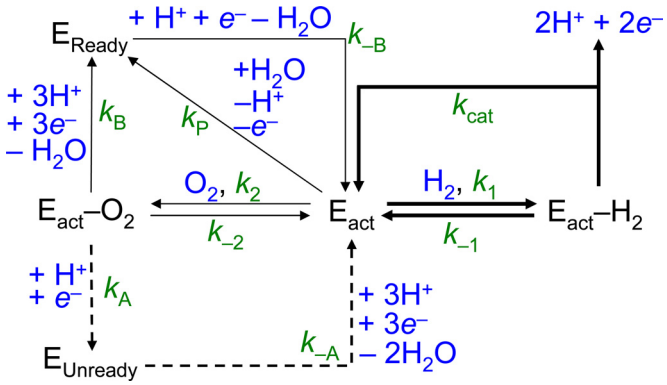


**Fig. 4.** The kinetic scheme used to model $O_2$ tolerance. *Re* MBH is abbreviated as "E" and is shown in the reduced active form ($E_{act}$), as an adduct with $H_2$ or $O_2$ ($E_{act}-H_2$ and $E_{act}-O_2$, respectively) or in the Ready ($E_{Ready}$) or Unready ($E_{Unready}$) state.

To bring these factors together, the catalytic cycle shown in Fig. 1*B* was modeled by using the kinetic cycle shown in Fig. 4 (*Re* MBH is represented by the symbol E). The steady-state approximation was applied to all intermediate species ($E_{act}-H_2$, $E_{act}-O_2$, $E_{Ready}$, and $E_{Unready}$). The following expression (Eq. **1**) was obtained (see *SI Appendix* for derivation), in which $K_M^{H_2}$ and $K_I^{O_2}$ are as defined in Eqs. **2** and **3**, respectively, and $i$ is the catalytic current.

$$\frac{i}{i_{max}} = \frac{\frac{K_I^{O_2}}{[O_2]}}{\frac{K_M^{H_2}}{[H_2]}\left(1+\frac{K_I^{O_2}}{[O_2]}+\frac{k_A}{k_{-A}}+\frac{k_B}{k_{-B}}\right)+\frac{K_I^{O_2}}{[O_2]}\left(1+\frac{K_M^{H_2}}{[H_2]}\frac{k_p}{k_{-B}}\right)} \quad [1]$$

$$K_M^{H_2} = \frac{k_{-1}+k_{cat}}{k_1} \quad [2]$$

$$K_I^{O_2} = \frac{k_{-2}+k_B+k_A}{k_2} \quad [3]$$

The term $K_I^{O_2}$ is the inhibition constant for $O_2$, and would vary from $K_I^{O_{2,app}}$ by a factor of $\{[H_2]/K_M^{H_2} \times (1+K_M^{H_2}/[H_2])\}$, if $O_2$ were to be considered simply as a competitive inhibitor.

Eq. **1** was fitted to the data to determine $K_I^{O_{2,app}}$ as described above at 10° C (pH 5.5, +0.122 V). Values of $k_{cat}$ (≈250 $s^{-1}$) and $k_{-A}$, the rate of reactivation of Unready (≈0.00025 $s^{-1}$) were used as "best guesses", based on analogy with standard [NiFe]-hydrogenases. The value of $k_P$, the rate of anaerobic inactivation, is ≈0.003 $s^{-1}$ at 10° C and is potential independent (see Fig. S2 of the *SI Appendix*). The value of $k_{-B}$, the rate of reactivation of Ready (≈0.03 $s^{-1}$) was determined under these conditions (Fig. 3). To simplify, the approximation was made that the rates of access of $H_2$ and $O_2$ ($k_1$ and $k_2$, respectively) depend only on their masses according to the kinetic theory of gases ($v_{H2}/v_{O2} = \sqrt{[mass_{O_2}/mass_{H_2}]}$), and hence $k_1 = 4 \times k_2$, and, for the reverse reaction, $k_{-1} = 4 \times k_{-2}$. Taking typical values of $K_M^{H_2}$ ≈4 μM and $K_I^{O_{2,app}}$ ≈60 μM at these conditions, the best fit to the experimental data (Fig. 5*A*) yielded $k_1 = 68\ \mu M^{-1}\ s^{-1}$, $k_{-1} = 22\ s^{-1}$ and the rate of formation of Ready from the initial $O_2$ adduct, $k_B = 0.01\ s^{-1}$.

The model allows an understanding of the roles of the different rate constants in affecting $O_2$ tolerance. Fig. 5*B* shows

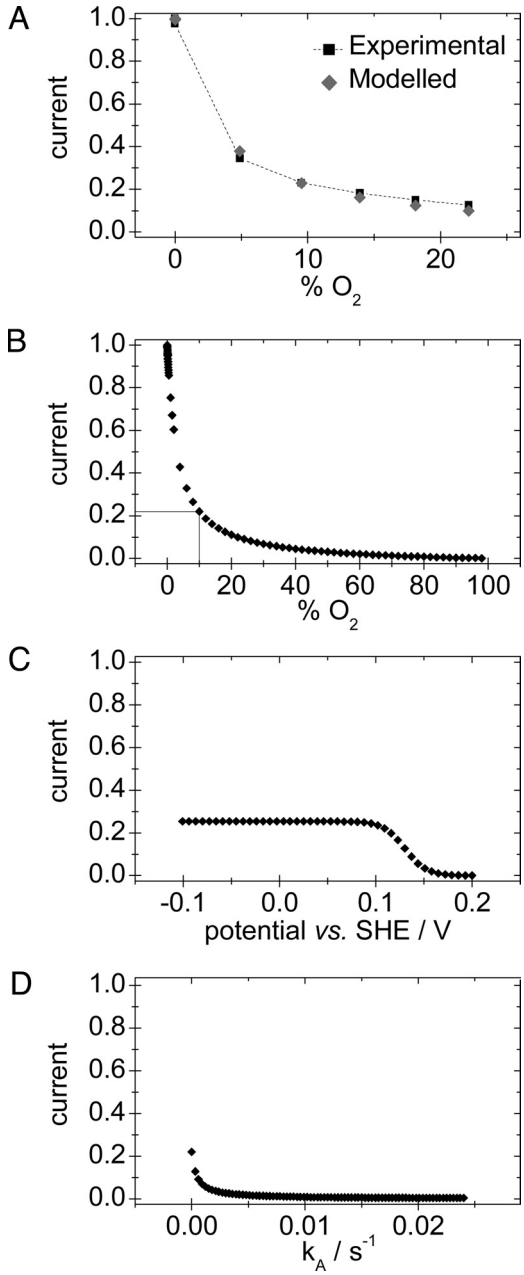


**Fig. 5.** Simulations obtained by applying Eq. **1** to *Re* MBH. (*A*) Limiting $H_2$ oxidation currents at varying $O_2$ concentrations, determined experimentally (black) and calculated from the model (gray). (*B–D*) show the effect of altering the percentage $O_2$ (*B*), the electrode potential (*C*), and $k_A$ (*D*) on the catalytic currents calculated from the model. All conditions are pH 5.5, 10° C. *B* and *D* are at 0.122 V, and *C* and *D* are at 10% $O_2$.

the effect of varying the $O_2$ concentration on the $H_2$ oxidation activity under the conditions above. Fig. 5*C* shows the effect of changing the electrode potential on the $H_2$ oxidation activity at 10% $O_2$; the potential dependence of $k_{-B}$ is modeled by using Eq. **4**. Fig. 5*D* stresses the importance, for $O_2$ tolerance, of not producing the Unready state, i.e., of ensuring that $k_A$ is very small. It is unclear as yet why *Re* MBH does not produce Unready, but formation of the Ready state ($k_B$) requires a greater immediate availability of electrons (and protons) than for producing the Unready state ($k_A$). This requirement could be accommodated by some property of *Re* MBH, such as an increase in the number of redox sites able to donate an electron.

Analogously, being embedded in the cytoplasmic membrane or immobilized on an electrode with a ready supply of electrons may protect the enzyme against $O_2$ inactivation.

$$k_{-B} = \frac{k_{-B,max}}{1 + \exp\left(\frac{2.3nF}{RT}(E - E^{\circ})\right)} \quad [4]$$

In essence, both the potential and temperature dependencies of $K_I^{O_2,app}$ emphasize the importance of enhancing the rate of recovery as opposed to limiting the rate of $O_2$ attack. Reactivation from Ready is faster at low potential and at high temperature, and this matches the characteristics of the $O_2$-tolerance factor. Interestingly, this means that *Re* MBH can be viewed as acting not only in $H_2$ cycling, but also as a very slow oxidase (20), catalyzing the four-electron reduction of $O_2$ to water with a rate constant in the order of $10^{-1}$–$10^{-2}$ $s^{-1}$. The positive temperature dependence could have particular significance for $O_2$-tolerant $H_2$ cycling in microorganisms such as *Aquifex aeolicus* (21), *Thermococcus litoralis* (22), and *Pyrococcus furiosus* (23) that live at high temperatures and could encounter $O_2$.

## Methods

The *Re* MBH enzyme was isolated and purified as described previously (15). All experiments were performed in an $N_2$-filled anaerobic glove box (M. Braun, <2 ppm $O_2$). A PGE rotating disk electrode (area 0.03 $cm^2$) was used with an electrode rotator (EcoChemie Autolab Rotator), which fitted tightly above a gas-tight, glass, electrochemical cell. A three-electrode configuration was used, with a Pt wire counter electrode and a saturated calomel reference electrode (SCE) located in a reference arm containing aqueous 0.10 M NaCl and connected to the working electrode compartment via a Luggin capillary. The temperature of the working compartment was controlled by using a water jacket, whereas the reference electrode remained at ≈25° C. The potential (*E*) was corrected with respect to the standard hydrogen electrode (SHE) by using the following formula: $E_{SHE} = E_{SCE} + 0.242$ V at 298 K (24): All potentials are quoted relative to SHE. An Autolab PGSTAT 10 electrochemical analyzer was used with an electrochemical detection module and GPES software (EcoChemie).

All experiments were carried out in 0.05 M sodium phosphate buffer with 0.10 M NaCl as supporting electrolyte (prepared by using purified water, 18.2 MΩ cm, Millipore) and titrated to the desired pH at the experimental temperature. Gases were of Premier/Research Grade and supplied by Air Products or BOC. Mass-flow controllers (Smart-Trak, Sierra Instruments) were used to supply precise mixtures of gases to the cell headspace at a constant flow rate.

To prepare films of MBH, the PGE electrode was polished by using an aqueous slurry of 1 μm α-alumina (Buehler) on cotton wool, then sonicated for *ca*. 5 s and rinsed with purified water, before 1.5 μl of enzyme solution (0.1–0.2 mg/mL) was successively applied and withdrawn from the electrode surface over a period of *ca*. 30 s. In all experiments, the electrode was rotated at a constant rate, typically 2,500 rpm, to provide efficient supply of substrate and removal of product from the electrode surface.

To measure $K_I^{O_2,app}$ and the rate of $O_2$ reaction, data were corrected for ''film loss'' over the course of the experiment by fitting anaerobic data points to a single exponential. A good fit was usually obtained (see Fig. 2) and by dividing the raw data by the exponential curve, normalized/corrected data were obtained. To obtain $K_I^{O_2,app}$, currents were corrected for film loss, and the inverse of the limiting value of the corrected current at each $O_2$ concentration was plotted against $O_2$ concentration, with $K_I^{2,app}$ given by dividing the *y* intercept by the gradient. Values of the Henry's constants for $H_2$ and $O_2$, and the temperature dependence thereof, were taken from ref. 25.

**Supporting Information.** Analysis of the rates of $O_2$ reaction, determination of the rate of anaerobic inactivation, and the derivation of Eq. **1**, are available in the *SI Appendix*.

**ACKNOWLEDGMENTS.** The authors wish to thank Dr. M. Ludwig for preparation of the membrane-bound uptake [NiFe]-hydrogenase samples, Dr. C. F. Blanford and Mr. P. A. Cracknell for help with modeling, and Dr. K. A. Vincent for obtaining preliminary results on the reactivation rates for *Ralstonia eutropha* MBH. J.A.C., A.F.W., and F.A.A. are supported by the Engineering and Physical Sciences Research Council UK (Grant Supergen 5) and the Biotechnology and Biological Sciences Research Council UK (Grant BB/D52222X/1). B.F. and O.L. are supported by the Sonderforschungsbereich (Grant 498, Project C1) and the Cluster of Excellence "Unicat" from the Deutsche Forschungsgemeinschaft.

1. Thauer RK, Klein AR, Hartmann GC (1996) Reactions with molecular hydrogen in microorganisms: Evidence for a purely organic hydrogenation catalyst. *Chem Rev* 96:3031–3042.
2. Vincent KA, Parkin A, Armstrong FA (2007) Investigating and exploiting the electrocatalytic properties of hydrogenases. *Chem Rev* 107:4366–4413.
3. Fontecilla–Camps JC, Volbeda A, Cavazza C, Nicolet Y (2007) Structure/function relationships of [NiFe]- and [FeFe]-hydrogenases. *Chem Rev* 107:4273–4303.
4. Volbeda A, et al. (2005) Structural differences between the Ready and unReady oxidized states of [NiFe] hydrogenases. *J Biol Inorg Chem* 10:239–249.
5. Ogata H, et al. (2005) Activation process of [NiFe] hydrogenase elucidated by high-resolution X-Ray analyses: Conversion of the Ready to the Unready state. *Structure* 13:1635–1642.
6. Goldet G, et al. (2008) Hydrogen production under aerobic conditions by membrane-bound hydrogenases from *Ralstonia* species. *J Am Chem Soc* 130:11106–11113.
7. Vincent KA, et al. (2005) Electrocatalytic hydrogen oxidation by an enzyme at high carbon monoxide or oxygen levels. *Proc Natl Acad Sci USA* 102:16951–16954.
8. Cracknell JA, et al. (2008) Enzymatic oxidation of $H_2$ in atmospheric $O_2$: The electrochemistry of energy generation from trace $H_2$ by aerobic microorganisms. *J Am Chem Soc* 130:424–425.
9. Conrad R (1996) Soil microorganisms as controllers of atmospheric trace gases ($H_2$, CO, $CH_4$, OCS, $N_2O$, and NO). *Microbiol Rev* 60:609–640.
10. Cracknell JA, Vincent KA, Armstrong FA (2008) Enzymes as working or inspirational electrocatalysts for fuel cells and electrolysis. *Chem Rev* 108:2439–2461.
11. Vincent KA, et al. (2006) Electricity from low-level $H_2$ in still air—an ultimate test for an oxygen tolerant hydrogenase. *Chem Commun* 5033–5035.
12. Duche O, Elsen S, Cournac L, Colbeau A (2005) Enlarging the gas access channel to the active site renders the regulatory hydrogenase HupUV of *Rhodobacter capsulatus* $O_2$ sensitive without affecting its transductory activity. *Febs J* 272:3899–3908.
13. Saggu M et al. (2009) Spectroscopic insights into the oxygen-tolerant membrane-associated [NiFe]-hydrogenase of *Ralstonia eutropha* H16. *J Biol Chem* 284:16264–16276.
14. Léger C, et al. (2004) Inhibition and aerobic inactivation kinetics of *Desulfovibrio fructosovorans* NiFe hydrogenase studied by protein film voltammetry. *J Am Chem Soc* 126:12162–12172.
15. Ludwig M, et al. (2009) Oxygen-tolerant $H_2$ oxidation by membrane-bound [NiFe]-hydrogenases of *Ralstonia* species: Coping with low-level $H_2$ in air. *J Biol Chem* 284:465–477.
16. Lamle SE, Albracht SP, Armstrong FA (2005) The mechanism of activation of a [NiFe]-hydrogenase by electrons, hydrogen, and carbon monoxide. *J Am Chem Soc* 127:6595–6604.
17. Pershad HR, et al. (1999) Catalytic electron transport in *Chromatium vinosum* [NiFe]-Hydrogenase: Application of voltammetry in detecting redox- active centers and establishing that hydrogen oxidation is very fast even at potentials close to the reversible $H^+/H_2$ value. *Biochem* 38:8992–8999.
18. Vincent KA, et al. (2005) Electrochemical definitions of $O_2$ sensitivity and oxidative inactivation in hydrogenases, *J Am Chem Soc* 127:18179–18189.
19. Burgdorf T, et al. (2005) The soluble $NAD^+$-reducing [NiFe]-hydrogenase from *Ralstonia eutropha* H16 consists of six subunits and can be specifically activated by NADPH. *J Bacteriol* 187:3122–3132.
20. Armstrong FA, et al. (2009) Dynamic electrochemical investigations of hydrogen oxidation and production by enzymes and implications for future technology. *Chem Soc Rev* 38:36–51.
21. Guiral M, Aubert C, Giudici–Orticoni MT (2005) Hydrogen metabolism in the hyperthermophilic bacterium *Aquifex aeolicus. Biochem Soc Trans* 33:22–24.
22. Rakhely G, Zhou ZH, Adams MW, Kovacs KL (1999) Biochemical and molecular characterization of the [NiFe] hydrogenase from the hyperthermophilic archaeon, *Thermococcus litoralis*. *Eur J Biochem* 266:1158–1165.
23. Baker SE, et al. (2009) Hydrogen production by a hyperthermophilic membrane-bound hydrogenase in water-soluble nanolipoprotein particles. *J Am Chem Soc* 131:7508–7509.
24. Bard A, Faulkner L (2001) *Electrochemical Methods*: *Fundamentals and Applications* (Wiley, New York).
25. Sander R (1999) Compilation of Henry's law constants for inorganic and organic species of potential importance in environmental chemistry (Version 3). Available at www.henrys-law.org. Accessed May 29, 2009.